Synthesis, Characterization, and Antibacterial Activity of Lanthanide Metal Complexes with Schiff Base Ligand Produced from Reaction of 4,4-Methylene Diantipyrine with Ethylenediamine

Kawther Adeeb Hussein* and Naser Shaalan

Department of Chemistry, College of Science for Women, University of Baghdad, Iraq

*** Corresponding author:**

tel: +964-7805758871
email: kawtheradeeb2015@gmail.com

Received: April 20, 2022
Accepted: July 19, 2022

DOI: 10.22146/ijc.74214

Abstract: *An environmentally friendly method for the synthesis of Schiff bases was described by combining 4,4-methylenediantipyrine with ethylenediamine. The complex was prepared in a classical way, the usual condensation reaction method. A series of metal complexes were prepared from reactions of lanthanide nitrate salts [Nd^{+3}, La^{+3}, Er^{+3}, Gd^{+3}, and Dy^{+3}] with a Schiff base ligand. The structures of the complexes were confirmed by analytical studies, spectral measurements, and thermal studies, and the prepared ligand was characterized using microanalysis technique, UV-Visible, infrared, nuclear magnetic resonance ^{1}H-NMR and ^{13}C-NMR, mass spectrometry, and thermogravimetric analysis (TGA), and the addition of conductivity measurement and magnetic moment of complexes. The results showed that these complexes have a consistency of 10 in which the elements are bonded with the ligand through the two nitrogen atoms at C=N and that the bonding ratio between the metal:ligand is in 1:2 ratio. By using agar disc-spreading, we tested several* in vitro *compounds for their antibacterial activity against four pathogenic bacteria, including* Staphylococcus aureus, Bacillus subtilis, Escherichia coli, *and* Klebsiella pneumoniae. *The majority of the complexes demonstrated antibacterial activity.*

Keywords: *Schiff's bases; lanthanide complexes; biological activity; 4,4-methylenediantipyrine*

INTRODUCTION

The lanthanide (III) ions (rare earth metal ions) coordination chemistry field is rapidly expanding because of its application in fundamental and applied research in a variety of fields ranging from chemistry to material science and biology [1-3]. The chemistry of Schiff base complexes with lanthanide has gained importance recently because of the vast range of applications of lanthanide complexes, such as in photochemistry and medicine [4-5]. The lanthanides are a series of 15 rare earth elements starting from cerium to lutetium in the Periodic Table with atomic numbers 58 through 71. Some scientists have added to them the element lanthanum 57, which precedes them in the Periodic Table, and the name of the lanthanide series is due to the element lanthanum [6-7]. The lanthanide series consists of a series of successive elements in which the f orbital is partially or filled with electrons, and the outer orbital is empty [8]. These elements overcome in their compounds the oxidation state +3, and in some of them, the +2 and +4 states appear, and the +3 state is the only stable state in lanthanum, gadolinium, and lutetium because it corresponds to the vacancy of the 4f orbital in it and its half-filling, and then it is completely filling [9-11]. While these metals can be considered transitional elements, they have properties that distinguish them from the rest of the elements [12].

One of the properties of the lanthanides that affect how they interact with other elements is the alkalinity property, which is the extent to which the atom can lose electrons [13]. Schiff base compounds are azomethine-containing compounds formed through a condensation reaction between primary amine and carbonyl compounds, and they were first reported by Hugo Schiff in 1864 [14-16]. Schiff base compounds are a significant and well-studied class due to their wide variety of biological uses, simplicity of manufacturing, chelating properties, and stability [17-19]. In addition to their unique properties and practical uses, Schiff bases are also particularly fascinating compounds that shield metal ions from the chemical environment by creating kinetically inert complexes. Additionally, they have a remarkable ability to organize lanthanide ions, and antipyrine derivatives possess certain scientific advantages [20-22]. Several lanthanide coordination compounds have been demonstrated to contain ligands containing nitrogen donor atoms that serve as good building blocks for creating other lanthanide coordination compounds. As a linkage in metal coordination chemistry, Schiff bases continue to play a significant role [23-24]. Schiff base metal complexes have played a significant role in the history of coordination chemistry, resulting in a wide range of articles ranging from pure synthetic efforts to contemporary studies of metal complexes on a physical, chemical, and biological level [25-26]. The objectives of this study are synthesizing a new Schiff base ligand from antipyrine derivatives which is (4,4-methylene diantipyrine), characterizing it by spectroscopic methods, synthesizing some complexes using salts of rare earth metal ions (Nd^{+3}, La^{+3}, Er^{+3}, Gd^{+3}, and Dy^{+3}), characterizing them by physical and spectral analytical methods, and studying their biological activity [27].

■ EXPERIMENTAL SECTION

Materials

All reagents and chemicals used in this study are in the analytical grade and purchased from Sigma-Aldrich such as 4,4-methylenediantipyrine (97%), ethylenediamine (99%), absolute ethanol (99%), and lanthanide nitrate $[Ln(NO_3)_3]{\cdot}6H_2O$ whereas Ln^{+3} = La, Nd, Er, Gd, and Dy.

Instrumentation

The microanalysis element of the studied ligand and complexes was carried out with a Thermo Finnegan flash device in Syria Energy Centre. Infrared spectra of ligands and their complexes were recorded within the range 4000–250 cm^{-1} using a device of the type Shimadzu FTIR-spectrometer and using a KBr disk for ligands and CsI for complexes at the Department of Chemistry, College of Science, Baghdad University. Also, the ^{1}H-NMR and ^{13}C-NMR spectra of the prepared ligand were recorded by using a Bruker 400 MHz AVANCE spectrometer after dissolving it with DMSO-d_6 solvent and using $Si(CH_3)_4$ (TMS) as a reference for measurement at room temperature in Ankara, Turkey, and the mass spectra of the prepared compounds were recorded by a Network Mass Selective device at the University of Ankara, Turkey. The melting point of the prepared ligand and their complexes using a device from the English company Stuart with a temperature range of 300 °C at the Department of Chemistry, College of Science, Baghdad University.

Procedure

Synthesis Schiff base of ligand

Schiff's base ligand was prepared by dissolving 1 g (1 mol) of 4,4-methylenediantipyrine in (20 mL) of ethanol absolute 99.9% in a round-bottom flask with a capacity of 100 mL. An amount of 0.154 g (1 mmol) of ethylenediamine in a separating funnel was added dropwise into the mixture, followed by 3–5 drops of glacial acetic acid with continuous stirring until the components were homogenous. The mixture was heated and refluxed for 4–6 h, at 100 °C. After the precipitation was completed, the white crystals were collected by filtration, washed with absolute ethanol, dried for 24 h, and then recrystallized in absolute hot ethanol. The re-crystallized powder was collected by filtration and then dried for 12 h. It had 75% yield and a melting point (m.p) 189–191 °C. The ligand was characterized by several techniques [28].

Preparation of lanthanide complexes

Lanthanide complexes are prepared by dissolving 0.1 g of Schiff bases ligand in 5 mL of methanol absolute in a 25 mL round bottom flask. An amount of 5 mL of methanol absolute at a time was added with lanthanides salts. The mixture was refluxed, stirred for 4 to 7 h, and then left to precipitate. Then the precipitate was collected and purified with water and ether and let dry to obtain a pure precipitate; the molar ratio was fixed at 1:2 [29].

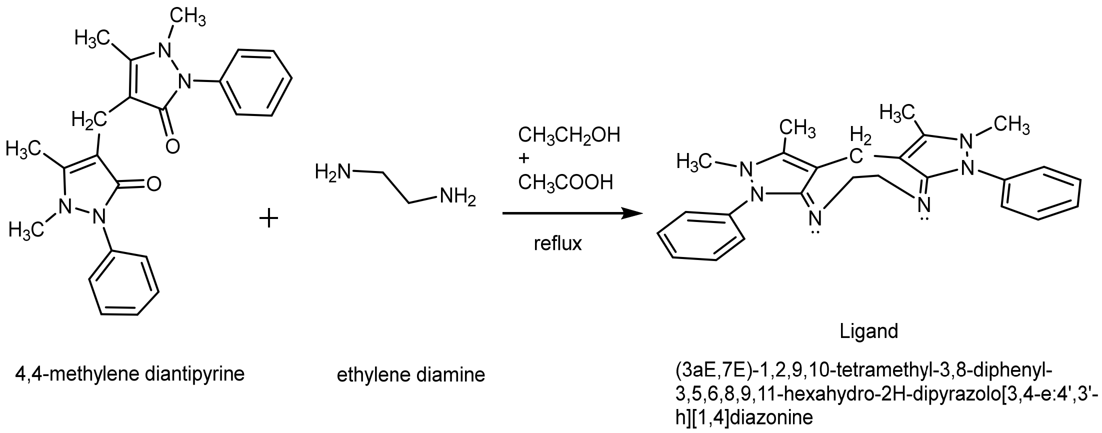

Scheme 1. The prepared Schiff base ligand

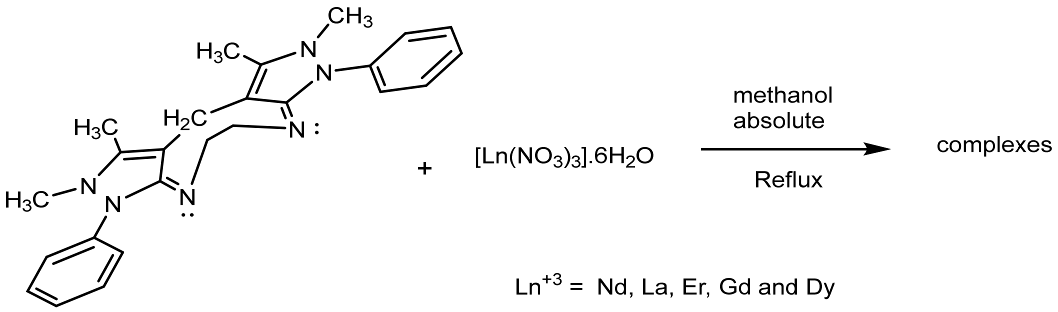

Scheme 2. Preparation of lanthanide complexes

Table 1. Microanalysis elements C, H, N, and O and physical data for ligand as well as its lanthanide complexes

Compound	M.wt	Yield%	Analysis (calculated)			
			C%	H%	N%	O%
L/[$C_{25}H_{28}N_6$]	412.54	75%	72.79 (73.02)	6.84 (6.79)	20.37 (19.95)	--
$C_{50}H_{56}N_{15}NdO_9$	1155.34	65%	51.98 (52.34)	4.89 (4.92)	18.19 (17.95)	12.46 (12.53)
$C_{50}H_{56}N_{15}LaO_9$	1150.00	60%	52.22 (52.34)	4.91 (4.82)	18.27 (17.95)	12.52 (12.67)
$C_{50}H_{56}N_{15}ErO_9$	1178.35	68%	50.97 (51.23)	4.79 (4.58)	17.83 (17.92)	12.22 (12.40)
$C_{50}H_{56}N_{15}GdO_9$	1168.34	65%	51.40 (52.13)	4.83 (3.97)	17.98 (17.89)	12.32 (12.72)
$C_{50}H_{56}N_{15}DyO_9$	1173.62	65%	51.17 (51.42)	4.81 (4.63)	17.90 (17.57)	12.27 (12.59)

■ RESULTS AND DISCUSSION

The reaction of the Schiff base ligand with the lanthanide nitrate [$Ln(NO_3)_3$]·$6H_2O$, Ln = La^{+3}, Nd^{+3}, Er^{+3}, Gd^{+3}, and Dy^{+3} produced good yields of complexes. The analytical data, along with some physical properties of the ligand and its metal complexes, are listed in Table 1.

FTIR Spectra of Schiff Bases Ligand

The Schiff bases ligand [$C_{25}H_{28}N_6$] was characterized using an FTIR spectrum as shown in Fig. S1, which revealed bands 3441, 3043, 2908, 1643, and 1589 cm^{-1} that are attributed to ν(O-H), hydrated water [30], ν(C-H) Aromatic, ν(C-H) (Aliph), ν(C=N), and ν(C=C) [31].

Mass Spectrum of Ligand

In coordination chemistry, mass spectroscopy is increasingly being used as a potent structural characterization tool. Mass spectra fragmentation patterns for free Schiff base ligand [$C_{25}H_{28}N_6$] were in good agreement with the structure in Fig. S2. The mass spectrum was characterized by an intense peak at 412.54 *m/z*, which corresponds to its molecular weight computed at 411.79 *m/z* [32].

Nuclear Magnetic Resonance Spectrum

^{1}H-NMR spectrum of ligand

The ^{1}H-NMR of protons was studied in DMSO-d_6 as the solvent and TMS as the standard reference. The spectrum of ligand showed a chemical shift at δ = 1.77, 2.23, and 2.51 ppm, which appeared to return to -CH_2-, -CH_3, and –CH_2- proton, respectively, in the 4-amino antipyrine and ethylenediamine compounds. The spectrum displayed various signals at δ = 7.34 and 7.48 ppm assigned into aromatic protons. In comparison, the beam appeared to return to N-CH_3 at the chemical shift at δ = 3.12 ppm; the chemical shift of the azomethine group C=N is not observable from ^{1}H-NMR because no proton is present related to the carbon azomethine group, the signals at δ = 2.32 and 2.97 ppm indicated into DMSO-d_6 and water (H_2O), respectively [33-34]. The ligand ^{1}H-NMR spectrum is shown in Fig. S3.

^{13}C-NMR spectrum of ligand

The ^{13}C-NMR was studied in DMSO-d_6 as the solvent. The spectrum of ligand showed CH_2 aliphatic at 11.48 ppm, -CH_3 at the 15.52 ppm, CH_3 and CH_2 at the aliphatic, N-CH_3 and N-CH_2 at 35.39, 40.02 at the CH. CH_2 at the aliphatic, CH-N-N at the 135.97 ppm, and the C-CH_3 at 155.33 ppm, while C=N at the 165.76 ppm [35], as shown in Fig. S4.

FTIR Spectra of Complexes

Infrared spectra were recorded for the ligand ($C_{25}H_{28}N_6$) in the range of 4000–400 cm^{-1} and its complexes in the range of 4000–200 cm^{-1}. The absorbance peaks of the IR spectra are summarized in Table 2, and representative IR spectra of the La complex are shown in Fig. S5. There was a distinct difference between the spectra of the complexes and the spectrum of the ligand due to its intensity and location. Further to that, it appeared that new bands emerged as a result of coordination between the ligand and the ions of the internal elements (lanthanides). It was also noted that the spectra of the complexes are similar among themselves due to the presence of the same effects in the vibrations of the ligand, and the infrared spectrum indicates the presence of a band at 3441–3439 cm^{-1}; which is attributed to the stretching frequencies of the O-H bond of the moisture that appeared in the spectra of each of the ligands and its lanthanide complexes.

The spectrum of the ligand also showed a medium-intensity absorption band located at a frequency of 3043 cm^{-1} due to the vibration of the aromatic C-H band stretching and the aliphatic absorption band at the frequency of 2908 cm^{-1}. The spectrum of the ligand similarly showed a medium-intensity band at the frequency 1492 cm^{-1}, which is generated from the vibration of the stretch band C=C of episode 4-aminoantipyrene. The spectrum of the ligand likewise showed a band at the frequency 1589 cm^{-1} belonging to the frequencies of the azomethine group C=N, 1591, 1583, 1593, 1581, 1577, and 1578 cm^{-1}, respectively, due to their participation in the coordination process with the lanthanide ions and forming complexes $C_{50}H_{56}N_{15}NdO_9$, $C_{50}H_{56}N_{15}LaO_9$, $C_{50}H_{56}N_{15}ErO_9$, $C_{50}H_{56}N_{15}GdO_9$, and $C_{50}H_{56}N_{15}DyO_9$ bond through the free electron pair of one of the atoms of this group. Bands appeared in the spectra of complexes 565, 530, 574, 572, and 572 cm^{-1} back to frequencies (M-O), 503, 412, 505, 503, and 435 cm^{-1} back to frequencies (M-N),

Table 2. The infrared spectrum of the prepared ligand and lanthanide complexes

Ligand\Complexes	ν(O-H) H_2O	ν(C=N)	ν(C=C)	ν(NO_3)	ν(NO_3)	ν(NO_3)	ν(M-O)	ν(M-N)
L/[$C_{25}H_{28}N_6$]	3458	1643	1589	---	---	--	---	---
$C_{50}H_{56}N_{15}NdO_9$	3481	1643	1525	1490	1456	1311	582	453
$C_{50}H_{56}N_{15}LaO_9$	3477	1620	1585	1492	1458	1304	588	458
$C_{50}H_{56}N_{15}ErO_9$	3446	1618	1575	1490	1458	1303	592	459
$C_{50}H_{56}N_{15}GdO_9$	3448	1616	1566	1490	1440	1300	590	435
$C_{50}H_{56}N_{15}DyO_9$	3446	1616	1560	1496	1458	1303	592	424

respectively, which is the result of forming coordination bonds between the donating atoms O and N with the central lanthanide ions [36-37].

Measurements with UV-Visible Spectroscopy

In Table 3, the UV-Vis spectra of the Schiff base ligand and its lanthanide complexes dissolved in DMSO (1×10^{-3} M) are listed. The absorption bands of ligand and two representative ions are shown in Fig. S6. The first high-intensity pack observed at λ_{max} = 283 was likely caused by the $\pi \rightarrow \pi^*$ transition of aromatic rings. The second absorption pack that appeared at λ_{max} = 290 nm corresponds to the $n \rightarrow \pi^*$ transition of the carbonyl group (C=O), and the last band at λ_{max} = 328 nm could be attributed to the $n \rightarrow \pi^*$ transition of the azomethine group (C=N). The absorption spectra of all investigated lanthanide complexes differ from the free Schiff base ligand in intensity and pattern [38], indicating that the Schiff base ligand is coordinated with Ln^{+3} ions. Evidence of complexes is revealed with different absorption bands around 450–1100 nm [39] (Table 3). In spectral terms with the same configuration 4f, a transition occurs (f→f). As a result, there are very sharp spectral bands that are similar to those observed with free ions. This is related to the possibility of such transitions. As a consequence of the valence selection rule (Laporte), electrical dipole transitions are not allowed when the lanthanide ion is subjected to a ligand field. As a result of the center asymmetric interactions, the dipole transition becomes partially permissible [40].

Magnetic Measurements of Lanthanide Complexes

The response of the transition elements to magnetism increases with the increase in the number of single electrons in the shell. As for the response of the lanthanide ions, it is related to how the electrons move in the orbit, as it is in the depth of the atom, and thus the lanthanide elements depend on the 4f shell electrons, especially the single electrons. Among the direct results, $\mu_{eff} = \sqrt{4S(S+1) + L(L+1)}$, where the magnetic effect resulting from the movement of the electron in its orbit contributes to paramagnetic, next to the spinning movement of the electron S, while the transitional elements, the participation of the orbital movement, is neglected due to the interference with the electric field of the ocean. The effective magnetic moment (μ_{eff}) of the created complexes has demonstrated that all the prepared complexes, except lanthanum complexes, are paramagnetic. The findings were compared with the real values and were closely related to the calculated values [41], as shown in Table 3.

Molar Conductivity Measurement of Lanthanide Complexes

Table 3 shows that all the lanthanide complexes are non-conductive in dimethylformamide (DMF) solvent at a concentration of 1×10^{-3} M. It was revealed that nitrate ions do not exist outside the coordination sphere.

Thermogravimetric Analysis (TGA)

The results of TGA of La^{+3}, Nd^{+3}, Er^{+3}, Gd^{+3}, and Dy^{+3} complexes are given in Fig. S7 and Table 4. The thermograms have been carried out in the range of up to 700 °C at a heating rate of 10 °C/min in a nitrogen atmosphere. They show an agreement in weight loss between the results obtained from the thermal decomposition and the calculated values. It was observed that the ligand undergoes two stages of decomposition. In the range of 45–240 °C, the estimated mass loss was 13.5% (calculated at 13.8%). Due to the decomposition

Table 3. The physical data, molar conductivity, and electronic spectra for Schiff base ligand and lanthanide complexes

Compound	Dec Point (°C)	Color	Conductivity DMF ($Cm^2.ohm^{-1}.mol^{-1}$)	Absorption bonds (nm)	Assigned transition	Magnetic moment (B.M)
$L/[C_{25}H_{28}N_6]$	189–191	White crystals	---	283, 290, 328	$\pi \rightarrow \pi^*$, $n \rightarrow \pi^*$	----
$C_{50}H_{56}N_{15}NdO_9$	280	White	20	---	$^1S_0$	Dia
$C_{50}H_{56}N_{15}LaO_9$	> 300	Light yellow	30	584, 738, 803, 981	$^4I_{9/2} \rightarrow {}^4G_{5/2}$, $^4I_{9/2} \rightarrow {}^2P_{1/2}$, $^4I_{9/2} \rightarrow {}^2D_{7/2}$	2.67
$C_{50}H_{56}N_{15}ErO_9$	270	Misty rose	20	488, 521, 542, 652, 974	$^3H_4 \rightarrow {}^4I_{15/2}$, $^4I_{15/2} \rightarrow {}^4G_{11/2}$	7.54
$C_{50}H_{56}N_{15}GdO_9$	280	Sea shell	20	757, 806, 909	$^8S_{7/2} \rightarrow {}^6I_{7/2}$	2.46
$C_{50}H_{56}N_{15}DyO_9$	260	Light yellow	30	650, 982	$^5I_{11} \rightarrow {}^6H_{5/2}$, $^6H_{15/2} \rightarrow {}^6P_{5/2}$	3.84

Table 4. TGA data of Schiff bases ligand and its lanthanide complexes

Sample step	Temperature range °C	TG weight mass loss		Reaction	Sample step	Temperature range °C	TG weight mass loss		Reaction
		Calc%	Found %				Calc%	Found %	
L(I)	45–240	13.8	13.5	$C_2H_4N_2$	Er (I)	25–75	7.5	7.3	$5H_2O$
L(II)	240–510	67.5	67.7	$C_{17}H_{19}N_4$	Er (II)	80–230	10.0	9.6	$2NO_3$
--	--	--	--	--	Er (III)	230–415	35.6	36.8	$NO_3 + C_{25}H_{28}N_6$
--	--	--	--	--	Er (IV)	415–590	32.3	32.1	$C_{25}H_{28}N_6$
Final residual		18.5	18.6	C_6H_6	Final residual		14.5	14.2	ErO
Nd (I)	25–75	8.0	8.5	$6H_2O$	Gd (I)	30–75	7.4	7.0	$6H_2O$
Nd (II)	75–180	10.1	9.8	$2NO_3$	Gd (II)	75–225	9.9	9.7	$2NO_3$
Nd (III)	180–430	36.9	37.5	$NO_3 + C_{25}H_{28}N_6$	Gd (III)	225–440	37.2	37.1	$NO_3 + C_{25}H_{28}N_6$
Nd (IV)	430–620	33.0	32.5	$C_{25}H_{28}N_6$	Gd (IV)	440–575	32.5	32.3	$C_{25}H_{28}N_6$
Final residual		12.5	12.6	NdO	Final residual		13.0	13.5	GdO
La (I)	25–70	6.9	7.1	$5H_2O$	Dy (I)	25–70	5.4	5.6	$4H_2O$
La (II)	70–225	10.2	9.8	$2NO_3$	Dy (II)	70–215	10.0	9.6	$2NO_3$
La (III)	225–430	37.5	37.6	$NO_3 + C_{25}H_{28}N_6$	Dy (III)	215–420	37.2	37.0	$NO_3 + C_{25}H_{28}N_6$
La (IV)	430–595	32.5	32.7	$C_{25}H_{28}N_6$	Dy (IV)	420–590	32.4	32.5	$C_{25}H_{28}N_6$
Final residual		12.4	12.3	LaO	Final residual		15.0	15.2	DyO

of $C_2H_4N_2$ in the first step, the range 240–510 °C, the estimated mass loss was 67.7% (calculated 67.5%) due to the decomposition of the $C_{17}H_{19}N_4$ molecule. In the final stage, an estimated mass loss of 18.6% (calculation of 18.5%) was due to the loss of the C_6H_6 molecule with a complete analysis. The data supports the results of elemental analysis and confirms the suggested formula. The complexes shown in Scheme 3 showed common behavior as in the following steps to the lanthanide complexes, respectively, as shown in Table 4 and Fig. S7. The analysis of the lanthanide complexes showed that the dissociation process of the loss goes through several stages, and the process occurs through 3 steps, as in Scheme 3, and this is proof of good thermal stability, where the loss in the first step is hydrated water not coordinated, and this means that the water is out of coordination, in each stage losing part of its weight and liberating a specific compound of the complexes that have been prepared. The temperature ranges are different among them, causing these differences to disintegrate the ions formed by the complexes after the dissolution, the material remaining after the complex has been formed may belong to lanthanide oxide [42-43]. Based on the characterization, the complex structure of lanthanide ions may be presented in Fig. 1.

Study of Antibacterial Activity

The findings showed that the produced ligand and its constituents were biologically efficient since the experiment was conducted in aerobic circumstances at 37 °C. Drilling was used to expose Schiff base ligand and lanthanide complexes to every pathogenic active of

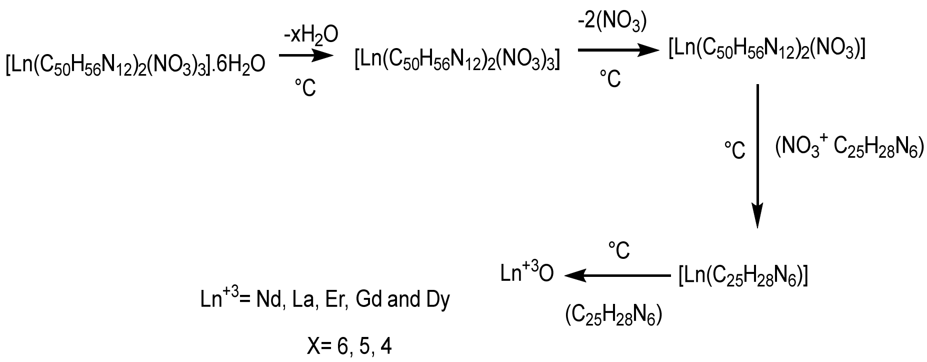

Scheme 3. TGA-analyses of lanthanide complexes

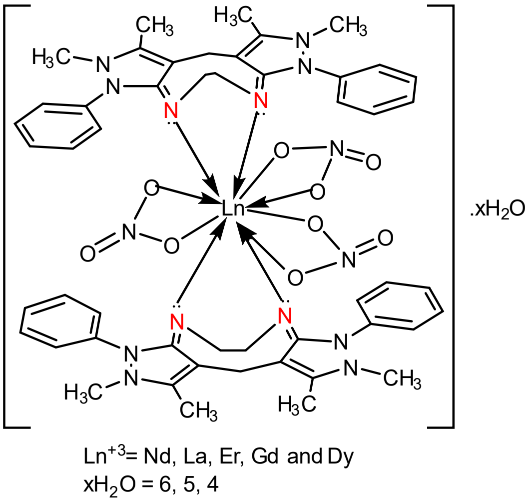

Fig 1. Suggested lanthanide complex structure with a coordination number of ten

pathogenic bacteria to four different types of pathogenic bacteria, i.e., two types of gram-negative bacteria: *Escherichia coli* and *Klebsiella pneumoniae*, and two gram-positive bacteria: *Staphylococcus aureus* and *Bacillus subtilis*. The complex was dissolved in DMF at 1 × 10^{-3} M concentration and they showed different efficacy to the negative and positive stain-bacteria of the complexes. The data is shown in Table 5, Fig. 2 and 3.

We conclude from the bacterial dishes that the ligand has variable biological activities, as it shows its activity for some types of bacteria and not for others, where it was found that the lanthanide complexes are

Table 5. The antibacterial activity of the prepared Schiff bases ligand and lanthanide compound

Sample	*S. aureus*	*B. subtilis*	*E. coli*	*K. penumoniae*
DMSO	–	–	–	–
L/[$C_{25}H_{28}N_6$]	++	+	–	+++
$C_{50}H_{56}N_{15}NdO_9$	++++	+	–	+++
$C_{50}H_{56}N_{15}LaO_9$	++++	+	–	+++
$C_{50}H_{56}N_{15}ErO_9$	++++	+++	++	–
$C_{50}H_{56}N_{15}GdO_9$	++++	++++	+	–
$C_{50}H_{56}N_{15}DyO_9$	++++	+++	–	–

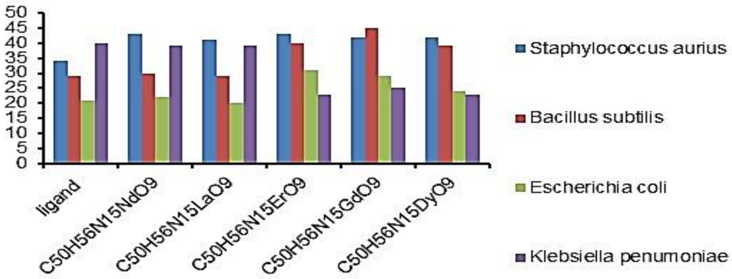

Fig 2. The chart shows the results of antibacterial biological activity of ligand and lanthanide complexes

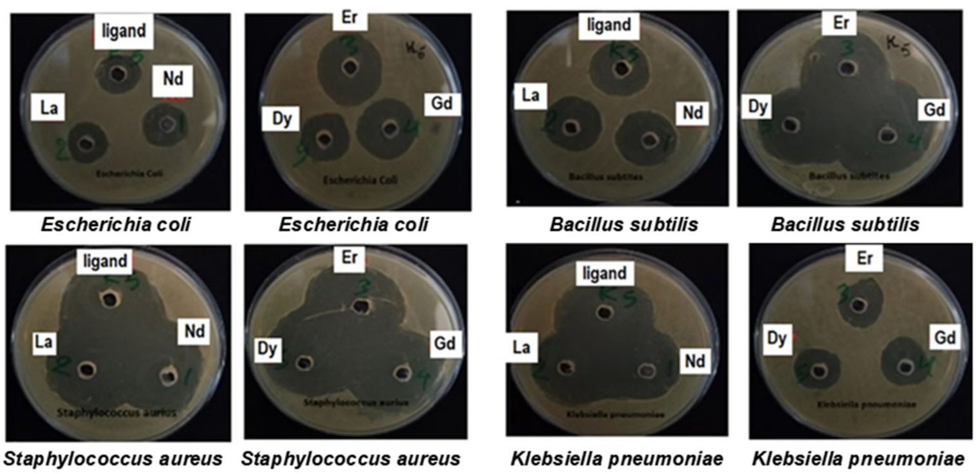

Fig 3. Biological activity of investigated compounds against *Escherichia coli, Klebsiella pneumoniae, Staphylococcus aureus*, and *Bacillus subtilis* for Schiff base ligand and its lanthanide complexes

more biologically active than the ligand due to the effect of the lanthanide elements, where the complexes showed more effective towards Gram-positive bacteria (*S. aureus*), followed by Gram-positive bacteria (*B. subtilis*), while Gram-negative bacteria show less activity than Gram-positive bacteria, especially (*E. coli*) where it shows less biological activity than (*K. pneumoniae*).

The created complexes are more efficient against Gram-positive bacteria (*S. aureus*). Gram-negative bacteria are more resistant due to the presence of a double membrane in each bacterial cell. Although all bacteria have an inner cell membrane, Gram-negative bacteria have a separate outer membrane. Some medicines and antibiotics are prevented from entering the cell by this outer layer [44]. Also, it turned out that the prepared compounds are antibacterial, positive, and negative for the Gram stain. We found that the prepared ligand is less effective than its complexes, and this is due to the small invasion that bacterial species show for such ions. The demise of bacterial species or the cessation of their growth can be through damage to the cell walls or prevention of the formation of the cell wall, or a decrease in the permeability of the cytoplasmic membranes, the physical and chemical composition of the protein, and nucleic acids in the cell, or cellular enzymatic activity, as well as through the prevention of manufacture of proteins and nucleic acids [45-47].

CONCLUSION

The Schiff-base ligand ((3a*E*,7*E*)-1,2,9,10-tetramethyl-3,8-diphenyl-3,5,6,8,9,11-hexahydro-2*H*-dipyrazolo[3,4-e:4',3'-h] [1,4]diazonine) obtained by condensation of 4,4-methyleneantipyrine with ethylenediamine and followed by the reaction with lanthanide(III) nitrate salts to form mononuclear complexes. The Schiff base ligand, on interaction with La^{+3}, Nd^{+3}, Er^{+3}, Gd^{+3}, and Dy^{+3}, yields compounds corresponding to the general formula $[Ln(L)_2(NO_3)_3]\cdot XH_2O$. [$Ln^{+3}$ = La, Nd, Er, Gd, and Dy, (X = 6, 5, 4)]. The analytical data showed that the metal-to-ligand ratio of the complexes is 2:1. At room temperature, spectroscopic studies, element microanalysis CHNO, molar conductivity, and magnetic moment measurements were used to describe these complexes. The compounds are crystalline complexes that disintegrate in four steps when heated in N_2 gas to 700 K. One of the results of thermal decomposition was that water is located outside the coordination field. As is the case in the structural complexes that were seen by four nitrogen atoms azomethine group and six oxygen from nitrate. The peaks of the infrared spectrum also support these findings. Furthermore, the thermal decomposition results support the assumptions we make about the complexes' structural features. The molecular ion peaks found in the ligand's mass spectra and peaks can be traced back to the products of possible ligand cleavage, which supports the structural formula of the ligand. There is no effect of the Schiff bases ligand on the 4f electrons of the lanthanide ions. The ligand and its metal complexes act as good effective biological activity using four types of bacteria which are two types of Gram-negative bacteria (*E. coli* and *K. pneumoniae*) and two Gram-positive bacteria (*S. aureus* and *B. subtilis*).

REFERENCES

[1] Paderni, D., Giorgi, L., Fusi, V., Formica, M., Ambrosi, G., and Micheloni, M., 2021, Chemical sensors for rare earth metal ions, *Coord. Chem. Rev.*, 429, 213639.

[2] Bünzli, J.C.G., 2014, Review: Lanthanide coordination chemistry: From old concepts to coordination polymers, *J. Coord. Chem.*, 67 (23-24), 3706–3733.

[3] Atwood, D.A., 2013, *The Rare Earth Elements: Fundamentals and Applications*, John Wiley & Sons, Hoboken, New Jersey, US.

[4] Alghool, S., Zoromba, M.S., and Abd El-Halim, H.F., 2013, Lanthanide amino acid Schiff base complexes: Synthesis, spectroscopic characterization, physical properties and *in vitro* antimicrobial studies, *J. Rare Earths*, 31 (7), 715–721.

[5] Chundawat, N.S., Jadoun, S., Zarrintaj, P., and Chauhan, N.P.S., 2021, Lanthanide complexes as anticancer agents: A review, *Polyhedron*, 207, 115387.

[6] Vernon, R.E., 2021, The location and composition of Group 3 of the periodic table, *Found. Chem.*, 23 (2), 155–197.

[7] Wedal, J.C., and Evans, W.J., 2021, A rare-earth metal retrospective to stimulate all fields, *J. Am. Chem. Soc.*, 143 (44), 18354–18367.

[8] Zasimov, P., Amidani, L., Retegan, M., Walter, O., Caciuffo, R., and Kvashnina, K.O., 2022, HERFD-XANES and RIXS Study on the electronic structure of trivalent lanthanides across a series of isostructural compounds, *Inorg. Chem.*, 61 (4), 1817–1830.

[9] Cotton, S., 2013, *Lanthanide and Actinide Chemistry*, John Wiley & Sons, Chichester, UK.

[10] Nehra, K., Dalal, A., Hooda, A., Bhagwan, S., Saini, R.K., Mari, B., Kumar, S., and Singh, D., 2022, Lanthanides β-diketonate complexes as energy-efficient emissive materials: A review, *J. Mol. Struct.*, 1249, 131531.

[11] Pari, G., Mookerjee, A., and Bhattacharya, A.K., 2005, First-principles electronic structure calculations of $R_3Al_5O_{12}$ (R being the rare-earth elements Ce–Lu), *Phys. B*, 365 (1-4), 163–172.

[12] Prats, H., and Stamatakis, M., 2022, Atomistic and electronic structure of metal clusters supported on transition metal carbides: Implications for catalysis, *J. Mater. Chem. A*, 10 (3), 1522–1534.

[13] Al-Qahtani, S.D., Alzahrani, S.O., Snari, R.M., Al-Ahmed, Z.A., Alkhamis, K., Alhasani, M., and El-Metwaly, N.M., 2022, Preparation of photoluminescent and photochromic smart glass window using sol-gel technique and lanthanides-activated aluminate phosphor, *Ceram. Int.*, 48 (12), 17489–17498.

[14] Malik, M.A., Dar, O.A., Gull, P., Wani, M.Y., and Hashmi, A.A., 2018, Heterocyclic Schiff base transition metal complexes in antimicrobial and anticancer chemotherapy, *MedChemComm*, 9 (3), 409–436.

[15] Patil, C.J., Patil, M.C., and Patil, M.C., 2019, Reduction of azomethine bond of organic compound: Part-2. Formation of aldimine and ketimine and their catalytic hydrogenation, *Int. J. Pharm. Biol. Arch.*, 10 (2), 134–137.

[16] Xu, Y., Shi, Y., Lei, F., and Dai, L., 2020, A novel and green cellulose-based Schiff base-Cu(II) complex and its excellent antibacterial activity, *Carbohydr. Polym.*, 230, 115671.

[17] Panda, J., Raiguru, B.P., Mishra, M., Mohapatra, S., and Nayak, S., 2022, Recent advances in the synthesis of imidazo[1,2-a]pyridines: A brief review, *ChemistrySelect*, 7 (3), e202103987.

[18] Soleimani, E., Taheri, S.A.N., and Sargolzaei, M., 2017, Synthesis, characterization, theoretical and biological studies of a new macrocycle Schiff base with Co(II), Ni(II), Cu(II) and Zn(II) complexes, *J. Chil. Chem. Soc.*, 62 (4), 3731–3740.

[19] Jirjees, V.Y., Suleman, V.T., Al-Hamdani, A.A., and Ahmed, S.D., 2019, Preparation, spectroscopic characterization and theoretical studies of transition metal complexes with 1-[(2-(1*H*-indol-3-yl)ethylimino)methyl]naphthalene-2-ol ligand, *Asian J. Chem.*, 31 (11), 2430–2438.

[20] Rasheed, A.M., Al-Bayati, S.M.M., Al-Hasani, R.A.M., and Shakir, M.A., 2021, Synthesizing, structuring, and characterizing bioactivities of Cr(III), La(III), and Ce(III) complexes with nitrogen, oxygen, and Sulpher donor bidentate Schiff base ligands, *Baghdad Sci. J.*, 18 (4), 1545–1551.

[21] Ajlouni, A.M., Abu-Salem, Q., Taha, Z.A., Hijazi, A.K., and Al Momani, W., 2016, Synthesis, characterization, biological activities and luminescent properties of lanthanide complexes with [2-thiophenecarboxylic acid, 2-(2-pyridinylmethylene)hydrazide] Schiff bases ligand, *J. Rare Earths*, 34 (10), 986–993.

[22] Al Zoubi, W., Mohamed, S.G., Al-Hamdani, A.A.S., Mahendradhany, A.P., and Ko, Y.G., 2018, Acyclic and cyclic imines and their metal complexes: Recent progress in biomaterials and corrosion applications, *RSC Adv.*, 8 (41), 23294–23318.

[23] El-Ansary, A.L., and Abdel-Kader, N.S., 2012, Synthesis, characterization of La(III), Nd(III), and Er(III) complexes with Schiff bases derived from benzopyran-4-one and thier fluorescence study, *Int. J. Inorg. Chem.*, 2012, 901415.

[24] Raczuk, E., Dmochowska, B., Samaszko-Fiertek, J., and Madaj, J., 2022, Different Schiff bases—Structure, importance and classification, *Molecules*, 27 (3), 787.

[25] Yusuf, T.L., Oladipo, S.D., Zamisa, S., Kumalo, H.M., Lawal, I.A., Lawal, M.M., and Mabuba, N., 2021, Design of new Schiff-base copper(II) complexes: Synthesis, crystal structures, DFT study, and binding potency toward cytochrome P450 3A4, *ACS Omega*, 6 (21), 13704–13718.

[26] Raman, N., Johnson Raja, S., and Sakthivel, A., 2009, Transition metal complexes with Schiff-base ligands: 4-Aminoantipyrine based derivatives–A review, *J. Coord. Chem.*, 62 (5), 691–709.

[27] Shaalan, N., Abed, A.Y., Alkubaisi, H.M., and Mahde, S., 2019, Synthesis, spectroscopy, biological activities and thermodynamic studies for new complexes of some lanthanide metals with Schiff's bases derived from [2-acetylth-iophene] with [2,5-dihydrazino-1,3,4-thiadiazole], *Res. J. Chem. Environ.*, 23, 181–187.

[28] Shaalan, N., Khalaf, W.M., and Mahdi, S., 2022, Preparation and characterization of new tetra-dentate N_2O_2 Schiff base with some of metal ions complexes, *Indones. J. Chem.*, 22 (1), 62–71.

[29] Shaalan, N.D., and Abdulwahhab, S.M., 2021, Synthesis, characterization and biological activity study of some new metal complexes with Schiff's bases derived from [*o*-vanillin] with [2-amino-5-(2-hydroxy-phenyl)-1,3,4-thiadiazole], *Egypt. J. Chem.*, 64 (8), 4059–4067.

[30] Martinez-Gomez, N.C., Vu, H.N., and Skovran, E., 2016, Lanthanide chemistry: From coordination in chemical complexes shaping our technology to coordination in enzymes shaping bacterial metabolism, *Inorg. Chem.*, 55 (20), 10083–10089.

[31] Akram, E., Shaalan, N., Rashad., A.A., Hasan, A., Al-Amiery, A., and Yousif, E., 2016, Study of structural and optical properties of new films derived PVC-2-[5-phenyl-1,3,4-thiadiazol-2-ylimino-methyl]-benzoic acid, *Res. J. Pharm., Biol. Chem. Sci.*, 7 (5), 2836–2844.

[32] Kareem, M.J., Al-Hamdani, A.A.S., Jirjees, V.Y., Khan, M.E., Allaf, A.W., and Al Zoubi, W., 2021, Preparation, spectroscopic study of Schiff base derived from dopamine and metal Ni(II), Pd(II), and Pt(IV) complexes, and activity determination as antioxidants, *J. Phys. Org. Chem.*, 34 (3), e4156.

[33] Obaid, S.M.H., Sultan, J.S., and Al-Hamdani, A.A.S., 2020, Synthesis, characterization and biological efficacies from some new dinuclear metal complexes for base 3-(3,4-dihydroxy-phenyl)-2-[(2-hydroxy-3-methylperoxy-benzylidene)-amino]-2-methyl propionic acid, *Indones. J. Chem.*, 20 (6), 1311–1322.

[34] Halli, M.B., and Sumathi, R.B., 2017, Synthesis, physico-chemical investigations and biological screening of metal (II) complexes with Schiff base derived from naphthofuran-2-carbohydrazide and citral, *Arabian J. Chem.*, 10, S1748–S1759.

[35] Sönmez, M., Sogukomerogullari, H.G., Öztemel, F., and Berber, İ., 2014, Synthesis and biological evaluation of a novel ONS tridentate Schiff base bearing pyrimidine ring and some metal complexes, *Med. Chem. Res.*, 23 (7), 3451–3457.

[36] Fouad, R., 2020, Synthesis and characterization of lanthanide complexes as potential therapeutic agents, *J. Coord. Chem.*, 73 (14), 2015–2028.

[37] Jawad, S.A.A., and Ahmed, H.A., 2021, Synthesis, characterization and study of amide ligand type N_2S_2 and metal complexes with di valance manganese, zinc and tri valance iron, *Ann. Rom. Soc. Cell Biol.*, 25 (3), 8511–8520.

[38] Kohale, R.L., Pawade, V.B., Dhoble, S.J., and Deshmukh, A.H., 2020, *Optical Properties of Phosphate and Pyrophosphate Compounds*, Woodhead Publishing, Sawston, UK.

[39] Al Zoubi, W., Kim, M.J., Yoon, D.K., Al-Hamdani, A.A.S., Kim, Y.G., and Ko, Y.G., 2020, Effect of organic compounds and rough inorganic layer formed by plasma electrolytic oxidation on photocatalytic performance, *J. Alloys Compd.*, 823, 153787.

[40] Hussein, K.A., and Shaalan, N., 2021, Synthesis, spectroscopy and biological activities studies for new complexes of some lanthanide metals with Schiff's bases derived from dimedone with 4-aminoantipyrine, *Chem. Methodol.*, 6 (2), 103–113.

[41] Satten, R.A., 1953, Analysis of the spectrum of the Nd^{+++} ion in the bromate crystal, *J. Chem. Phys.*, 21 (4), 637–648.
[42] Pallares, R.M., and Abergel, R.J., 2020, Transforming lanthanide and actinide chemistry with nanoparticles, *Nanoscale*, 12 (3), 1339–1348.
[43] Wanja, D.W., Mbuthia, P.G., Waruiru, R.M., Bebora, L.C., Ngowi, H.A., and Nyaga, P.N., 2020, Antibiotic and disinfectant susceptibility patterns of bacteria isolated from farmed fish in Kirinyaga county, Kenya, *Int. J. Microbiol.*, 2020, 8897338.
[44] Obaid, S.M., Jarad, A.J., and Al-Hamdani, A.A.S., 2020, Synthesis, characterization and biological activity of mixed ligand metal salts complexes with various ligands, *J. Phys.: Conf. Ser.*, 1660, 012028.
[45] Tavares, T.D., Antunes, J.C., Padrão, J., Ribeiro, A.I., Zille, A., Amorim, M.T.P., Ferreira, F., and Felgueiras, H.P., 2020, Activity of specialized biomolecules against gram-positive and gram-negative bacteria, *Antibiotics*, 9 (6), 314.
[46] Delcour, A.H., 2009, Outer membrane permeability and antibiotic resistance, *Biochim. Biophys. Acta, Proteins Proteomics*, 1794 (5), 808–816.
[47] Sherif, S.H., Kure, D.A., Moges, E.A., and Argaw, B., 2021, Synthesis, characterization, and antibacterial, activity, evaluation of 4-amino antipyrine derivatives and their transition metal complexes, *Am. J. Biosci. Bioeng.*, 9 (1), 8–12.